

Functional expression of PHO1 to the Golgi and *trans*-Golgi network and its role in export of inorganic phosphate

A. Bulak Arpat, Pasqualina Magliano, Stefanie Wege, Hatem Rouached, Aleksandra Stefanovic and Yves Poirier*

Department of Plant Molecular Biology, Biophore Building, University of Lausanne, CH-1015 Lausanne, Switzerland

Received 21 December 2011; revised 16 March 2012; accepted 21 March 2012; published online 25 May 2012.

*For correspondence (e-mail yves.poirier@unil.ch).

SUMMARY

Arabidopsis thaliana PHO1 is primarily expressed in the root vascular cylinder and is involved in the transfer of inorganic phosphate (Pi) from roots to shoots. To analyze the role of PHO1 in transport of Pi, we have generated transgenic plants expressing PHO1 in ectopic *A. thaliana* tissues using an estradiol-inducible promoter. Leaves treated with estradiol showed strong PHO1 expression, leading to detectable accumulation of PHO1 protein. Estradiol-mediated induction of PHO1 in leaves from soil-grown plants, in leaves and roots of plants grown in liquid culture, or in leaf mesophyll protoplasts, was all accompanied by the specific release of Pi to the extracellular medium as early as 2–3 h after addition of estradiol. Net Pi export triggered by PHO1 induction was enhanced by high extracellular Pi and weakly inhibited by the proton-ionophore carbonyl cyanide *m*-chlorophenylhydrazone. Expression of a PHO1-GFP construct complementing the *pho1* mutant revealed GFP expression in punctate structures in the pericycle cells but no fluorescence at the plasma membrane. When expressed in onion epidermal cells or in tobacco mesophyll cells, PHO1-GFP was associated with similar punctate structures that co-localized with the Golgi/*trans*-Golgi network and uncharacterized vesicles. However, PHO1-GFP could be partially relocated to the plasma membrane in leaves infiltrated with a high-phosphate solution. Together, these results show that PHO1 can trigger Pi export in ectopic plant cells, strongly indicating that PHO1 is itself a Pi exporter. Interestingly, PHO1-mediated Pi export was associated with its localization to the Golgi and *trans*-Golgi networks, revealing a role for these organelles in Pi transport.

Keywords: PHO1, Golgi, *trans*-Golgi network, phosphate, export, *Arabidopsis*.

INTRODUCTION

Ion homeostasis in eukaryotes depends on the controlled flux of ions in between cells and organs as well as across several subcellular compartments. Both uptake of ions into cells and their export out of cells are crucial for ion homeostasis in multicellular organisms. This is true for many of the major macronutrients, including inorganic phosphate (Pi). Well-known examples where Pi efflux is crucial for plant Pi homeostasis include the transfer of Pi into the root xylem from the surrounding vascular cells as well as the release of Pi at the periarbuscular interface of mycorrhizal roots (Poirier and Bucher, 2002; Bucher, 2006; Bonfante and Genre, 2010). Export of Pi and ions may also be physiologically relevant to cells that are symplastically isolated from the rest of the plant tissues, such as the guard cells, embryo and pollen grains. These cells must be able to acquire nutrients from the surrounding tissues via the apoplast (McLean *et al.*, 1997). Despite their importance, relatively little is known about the genes and proteins involved in mediating ion efflux, including Pi, in eukaryotic cells.

Only a few proteins have been identified that play an important role in the export of ions to the root xylem tissues. *SKOR1* is a member of the Shaker family expressed in the root stelar cells and encoding an outwardly rectifying K⁺ channel mediating loading of K⁺ in the xylem vessel (Gaymard *et al.*, 1998). Similarly, *BOR1* encodes a boron transporter expressed in the root stelar cells and mediating boron efflux into the xylem vessel (Takano *et al.*, 2002). *NRT1.5* is a bidirectional nitrate transporter and a knockout *nrt1.5* mutant has decreased transfer of nitrate from roots to shoot, suggesting a role in nitrate efflux to the xylem (Lin *et al.*, 2008).

The *Arabidopsis thaliana pho1* mutant is defective in the transfer of Pi from root to shoot, resulting in Pi-deficient shoots but Pi-sufficient roots (Poirier *et al.*, 1991). The *PHO1* gene is expressed primarily in the vascular tissue of the root and hypocotyl (Hamburger *et al.*, 2002) and the corresponding protein shows no homology to members of the plant PHT family, including the PHT1 H⁺/Pi co-transporters. PHO1

contains two domains, named SPX and EXS, that have been identified in some *Saccharomyces cerevisiae* and plant proteins involved in phosphate transport or sensing (Wang *et al.*, 2004; Chiou and Lin, 2011; Secco *et al.*, 2012). The *PHO1* gene family harbors 11 members in Arabidopsis and homologs are found throughout the plant kingdom, including monocots and mosses (Wang *et al.*, 2004, 2008; Secco *et al.*, 2010). Proteins homologous to *PHO1* are also present in a large spectrum of eukaryotes, from *Caenorhabditis elegans*, to Drosophila, to mammals, but no function for *PHO1* homologs outside the plant kingdom is known (Hamburger *et al.*, 2002).

No Pi transport activity has yet been demonstrated for *PHO1* via its expression in heterologous non-plant systems (including *Xenopus* oocytes, yeast and liposomes). It has recently been shown that constitutive over-expression of *PHO1* in the vascular cylinder of roots and shoots resulted in strongly reduced rosette growth, the accumulation of Pi in leaves and guttation fluid and the release of Pi from leaves into the perfusion medium (Stefanovic *et al.*, 2011). While these data strengthened the connection between *PHO1* and Pi loading to the vascular cylinder, it remained unknown whether the release of Pi to the perfusion medium was caused by the excessive shoot Pi accumulation and whether *PHO1* could mediate Pi export in ectopic cells with a normal physiological status.

In the current study, transgenic plants were produced in which *PHO1* was under the control of an inducible promoter regulated by estradiol. In these transgenic plants, *PHO1* could be over-expressed at determined times in plants that were phenotypically normal and in tissues other than the vascular cylinder. It was thus possible to demonstrate that expression of *PHO1* in leaf mesophyll protoplasts, a type of cell that does not normally express *PHO1*, leads to rapid and specific Pi export. Furthermore, transient expression of *PHO1* in tobacco via *Agrobacterium tumefaciens* infiltration also led to specific Pi release. Surprisingly, using a functional *PHO1-GFP* construct, *PHO1* was observed primarily in the Golgi and trans-Golgi network (TGN), as well as uncharacterized vesicular structures. Partial relocalization of *PHO1* to the plasma membrane (PM) could be induced only by a high level of phosphate. These data provide strong support that *PHO1* is itself a Pi exporter and highlight a role for the Golgi, TGN and the endo-trafficking system in Pi export.

RESULTS

Establishment of an estradiol-inducible *Pho1* expression system

The *PHO1* gene was put under the control of the OlexA promoter inducible by the presence of estradiol using the pMDC221 vector (Figure S1a in Supporting Information) (Brand *et al.*, 2006). Twelve independent transgenic lines transformed with the inducible *PHO1* construct were shown

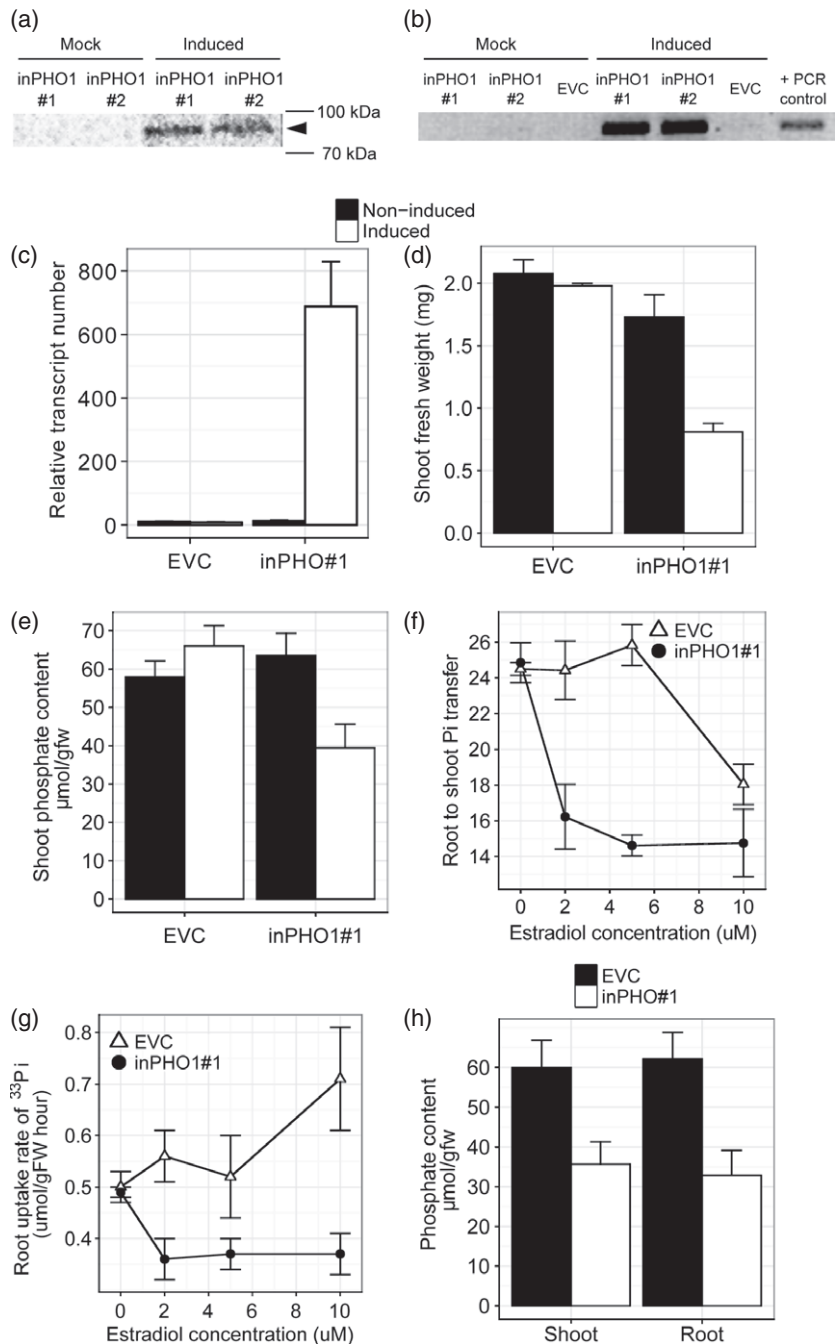
by RT-PCR to strongly over-express *PHO1* in whole seedlings only in the presence of estradiol and not with the mock control (data not shown). Based on these preliminary analyses, two independent lines with an inducible *PHO1* expression were analyzed in more detail, namely lines inPHO1#1 and inPHO1#2. A control line transformed with an empty vector was also included (line EVC). Leaves of soil-grown inPHO1 plants treated with a solution of estradiol showed a strong increase of *PHO1* expression, both at the mRNA and the protein level, compared either with leaves of the same plants treated with a mock solution or with leaves of transgenic EVC (Figure 1a,b). Quantitative RT-PCR showed that *PHO1* was over-expressed several hundred-fold in shoots treated with estradiol compared with either shoots treated with a mock solution or with leaves of transgenic EVC with or without inducer (Figure 1c).

The EVC or inPHO1 transgenic plants were indistinguishable from wild type (WT) when grown in soil or in agar-solidified half-strength Murashige and Skoog (MS) medium (Figures 1d and Figure S1b and data not shown). However, germination of seeds on agar-solidified medium containing estradiol led to a severe reduction in growth of inPHO1#1, while growth was normal for either the estradiol- or mock-treated EVC line, or the mock-treated inPHO1#1 lines (Figure 1d). The poor growth of the inPHO1 lines in the presence of estradiol was associated with reduced Pi content in shoots (Figure 1e). Interestingly, rates of both translocation of Pi from roots to shoots and Pi uptake by the root system were decreased by the induction of *PHO1* expression (Figure 1f,g). Consequently, accumulation of Pi in the roots as well as in the shoots was reduced by approximately 40–45% in inPHO1#1 line but not in the EVC line when grown under sufficient external Pi (1000 μM) supplemented with 5 μM estradiol (Figure 1h).

Export of Pi mediated by induction of *PHO1* in whole leaves and mesophyll protoplasts

To examine Pi export in leaves expressing *PHO1*, rosette leaves from inPHO1 and EVC plants were first mock-treated or inducer-treated for 12 h, leaves were then excised, immersed in a Pi-free solution and the amount of Pi released into the medium measured between 2 and 16 h. While negligible Pi release corresponding to less than 5% of the total intracellular Pi was measured in the induced or non-induced EVC plants as well as the non-induced inPHO1 plants, Pi release corresponding to 25–30% of the total intracellular Pi was measured in the induced inPHO1 lines (Figure 2a). Release of Pi in the perfusion medium was thus dependent on the induction of *PHO1* by estradiol and it was rapid, being clearly measurable 2 h after application of estradiol (Figure 2a). Export of Pi was also independent of the intracellular Pi level at the time of immersion in the perfusion medium (Figure 2b). In a separate experiment, the specificity of Pi export was examined for leaves that were treated with estradiol for 12 h followed by

Figure 1. Inducible expression of *PHO1* and its effects on seedlings. (a) Western analysis of leaves of two independent inducible *PHO1* lines (inPHO1#1 and #2). For each line, two leaves of a soil-grown plant were treated with 5 μ M estradiol (induced) while two other leaves were treated with mock solution for 12 h. (b) Reverse transcriptase-PCR of *PHO1* expression. Leaves from lines inPHO1 #1 and #2 and from an empty vector control (EVC) line were mock-treated or estradiol-treated as described in (a). The +PCR control lane was performed using a plasmid containing full-length *PHO1* genomic fragment. (c) Quantitative RT-PCR of *PHO1* expression in shoots of 10-day-old seedlings grown on half-strength MS plates containing 1 mM inorganic phosphate (Pi) and supplemented either with mock solution (non-induced) or 5 μ M estradiol (induced). Values represented are mean relative transcript number of *PHO1* normalized against the reference gene *At5g46630* (Czechowski *et al.*, 2005) ($n = 3$). (d) Shoot fresh weight and shoot phosphate content (e) of 10-day-old seedlings grown on half-strength MS plates containing 1 mM Pi and supplemented either with mock solution (non-induced) or 5 μ M estradiol (induced). A biological unit consisted of six or seven seedlings ($n = 3$). (f) Root-to-shoot transfer rate and (g) root uptake capacity. Nine-day-old seedlings grown on 0.5 \times MS (1 mM Pi) were transferred to 0.5 \times MS (50 μ M Pi) supplemented with different concentrations of estradiol and grown for an additional 3 days before Pi uptake and transfer assays. A biological unit consisted of three or four seedlings ($n = 4$). (h) Shoot and root phosphate content of 10-day-old seedlings grown on half-strength MS plates containing 1 mM Pi and 5 μ M estradiol. A biological unit consisted of five or six seedlings ($n = 4$). For each graph, error bars represent the standard error.



4 h immersion into a Pi- and nitrate-free medium. The strong Pi export in estradiol-induced inPHO1 plants was not accompanied by the export of nitrate (Figure 2c).

To test whether *PHO1* over-expression could mediate efflux of Pi from a more uniform population of cells that do not normally express *PHO1*, mesophyll protoplasts were prepared from leaves of inPHO1 and EVC lines, cells were suspended in a Pi- and nitrate-free medium containing either mock or estradiol solution and the export of Pi and nitrate was measured after 4 h. Only the estradiol-treated inPHO1 line

exported Pi into the perfusion medium without any significant changes in nitrate export (Figure 3). Altogether, these results showed that induction of *PHO1* expression triggers specific Pi export even in cells that do not normally express the gene to a significant extent, such as leaf mesophyll cells.

Influence of the extracellular medium on Pi export mediated by PHO1

In order to measure the influence of the extracellular medium on Pi export, we developed a simplified system in which

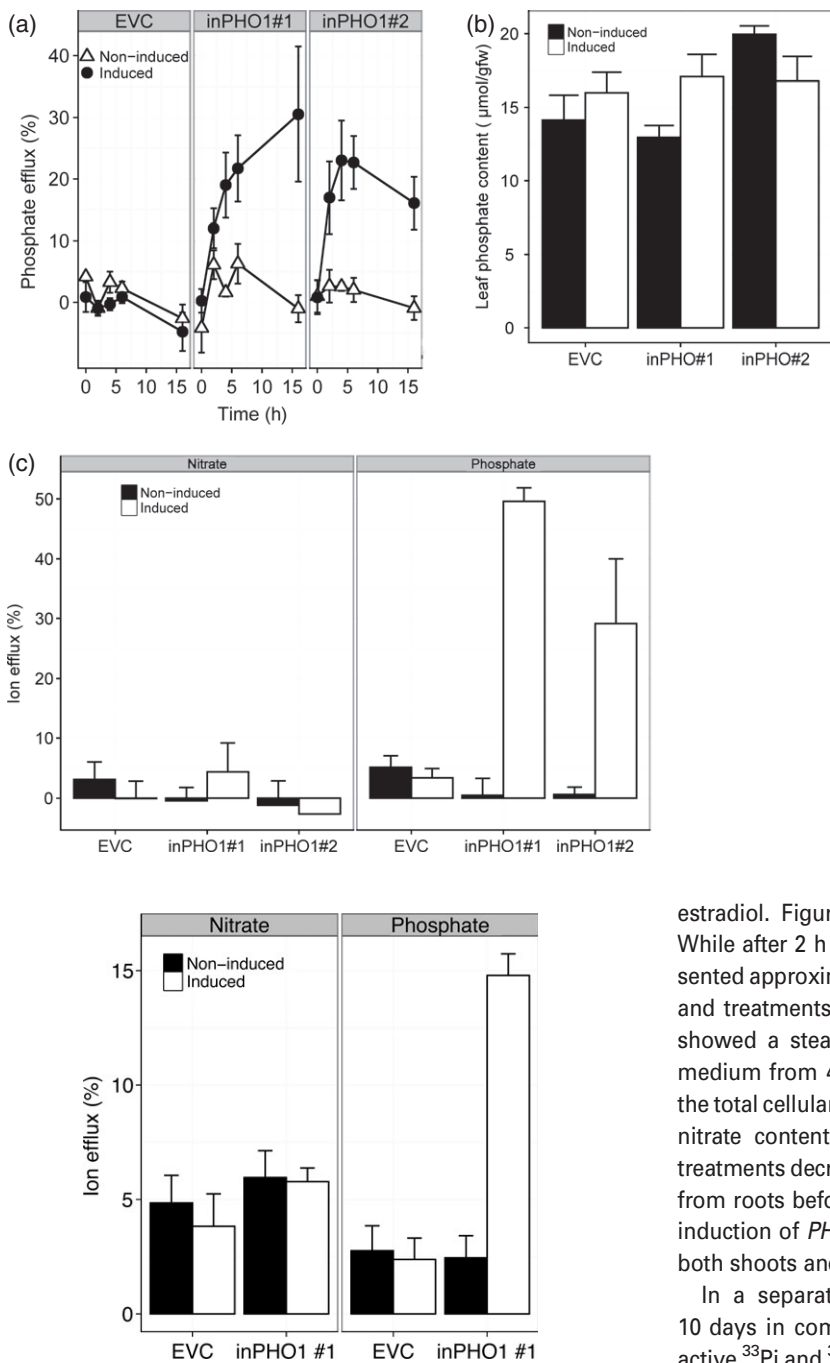


Figure 3. *PHO1*-dependent efflux of inorganic phosphate (Pi) from mesophyll protoplasts. Mesophyll protoplasts from empty vector control (EVC) and *PHO1*-inducible (inPHO1#1) lines were treated with 5 µM estradiol (induced) or mock solution (non-induced) for 3 h. After induction, Pi and nitrate in the solution were measured at 0 and 4 h. Efflux was expressed as average percentage of released Pi and nitrate to total Pi and nitrate, respectively, contained in protoplasts for each line after correcting for the initial ion concentration in the solution at 0 h. Error bars represent standard error ($n = 4$).

whole seedlings were grown for 10 days in MS liquid medium before being washed and immersed in a Pi- and nitrate-free medium and either mock-treated or treated with

Figure 2. *PHO1*-mediated export of inorganic phosphate (Pi) out of leaves.

(a) Leaves of two independent *PHO1*-inducible (inPHO1#1 and #2) and empty vector control (EVC) lines were treated with 5 µM estradiol (induced) or mock solution (non-induced), cut in small pieces and immersed into perfusion solution for 16 h. The phosphate concentration in the bathing solution was quantified every 2 h and expressed as percentage of total Pi contained in the leaf material for each sample. (b) Average phosphate content in the leaf samples used in (a) expressed as micromoles of Pi per gram fresh weight (µmol Pi/gfw). (c) Four or five leaves of soil-grown plants were either treated with mock solution or 5 µM estradiol on separate rosettes. After 12 h of induction, the mid-veins of the leaves were removed and samples were used to measure the Pi and nitrate released into the perfusion solution after 4 h of incubation. The Pi (right panel) or nitrate export (left panel) was expressed as percentage of total Pi or nitrate, respectively, contained in the leaf material for each sample. Error bars represent standard error ($n = 6$).

estradiol. Figure 4 shows the results of such experiment. While after 2 h the Pi content in the infiltration media represented approximately 2% of the cellular Pi content for all lines and treatments, only the inPHO1 line treated with estradiol showed a steady increase of Pi content in the infiltration medium from 4 h onwards, reaching approximately 12% of the total cellular Pi content after 8 h (Figure 4). In contrast, the nitrate content in the infiltration media for all lines and treatments decreased with time (Figure 4). Separating shoots from roots before mock or estradiol treatment revealed that induction of *PHO1* by estradiol resulted in export of Pi from both shoots and roots (Figure S2).

In a separate experiment, whole seedlings grown for 10 days in complete medium were pre-loaded with radioactive ^{33}P and ^{35}S before being switched to a Pi- and SO_4 -free medium and mock or estradiol treatment. After 12 h the Pi released reached 1.2% and 16% of total cellular ^{33}P for mock- and estradiol-treated plants, respectively, while released of ^{35}S remained low for both treatments, at 1.4% (Figure 5a). Thus, Pi export mediated by *PHO1* induction is not associated with SO_4 export.

The effects of the disruption of the proton gradient across membranes and of the external Pi concentration on *PHO1*-mediated Pi export was measured using whole plants grown in media with ^{33}P . While addition of 20 µM of the proton ionophore carbonyl cyanide *m*-chlorophenylhydrazone

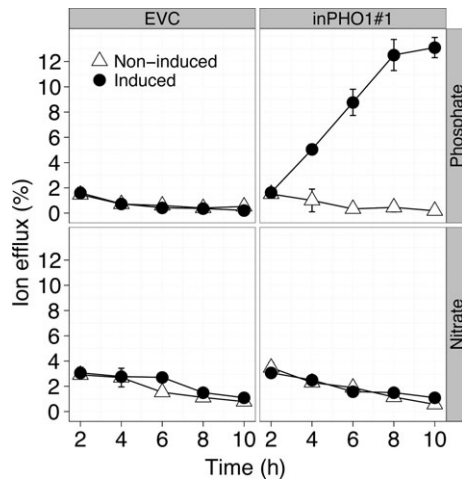


Figure 4. Export of inorganic phosphate (Pi) and nitrate in whole plants over-expressing *PHO1*. Plants from the empty vector control (EVC, left) and *PHO1*-inducible (inPHO1#1, right) lines were grown for 10 days immersed in liquid medium and then treated with 10 μM estradiol (induced) or mock solution (non-induced). The Pi (top) and nitrate (bottom) concentrations in the bathing solution were quantified every 2 h and expressed as percentage of total Pi or nitrate contained in plant material for each sample. Error bars represent standard deviation ($n = 4$).

(CCCP) reduced Pi uptake into plants by eight-fold compared with the control (Figure 5b), the same treatment led to only a small reduction in *PHO1*-mediated Pi export (Figure 5c). In contrast, raising the external Pi concentration from 50 μM Pi to 10 mM led to a two-fold increase in *PHO1*-mediated Pi export (Figure 5c). These results reveal that while Pi import into cells is highly dependent on the H^+ gradient across the PM and is modulated by external Pi concentration, Pi export mediated by *PHO1* expression is not influenced by these parameters to the same extent.

PHO1 is primarily localized to the golgi and TGN

A construct fusing GFP to the carboxy terminal end of *PHO1* was made, expressing the hybrid gene under the control of the endogenous *PHO1* promoter. Transformation of the *PHO1*-GFP construct in the *pho1-4* mutant led to phenotypic complementation at the level of rosette appearance, shoot fresh weight, shoot Pi content and root-to-shoot Pi transfer (Figure S3). The complemented *pho1-4* mutant showed *PHO1*-GFP expression primarily in the vascular cylinder of the root, with the strongest expression in the pericycle and cells associated with the xylem poles (Figure S4). At the subcellular level, *PHO1*-GFP expression was found associated with punctate bodies, and no fluorescence was found at the PM (Figure 6a). Two groups of bodies could be distinguished based on size: larger bodies with an average Feret diameter of 1.09 μm (SD = 0.16 μm , $n = 21$), and much smaller bodies whose size could not be determined within the limits of the microscopy configuration used (Fig-

ure 6a). Attempts to co-localize the fluorescence pattern to particular subcellular compartments by crossing the complemented *pho1-4* line with various lines expressing marker protein fused to mCherry failed (Geldner *et al.*, 2009). This failure was due to the combination of relatively weak expression and fluorescence of these marker-mCherry fusions in the vascular cylinder and difficulties in obtaining adequate resolution in a tissue as deep within the root as the pericycle, even when using a two-photon confocal microscope (data not shown). As an alternative, we used co-bombardment of onion epidermal cells with a combination of C-terminal *PHO1*-GFP and marker genes-mCherry fusions under the control of the CaMV35S promoter. Bombardment of the *PHO1*-GFP construct in onion cells produced a pattern of GFP expression in punctate bodies similar to the pattern observed in Arabidopsis roots (Figure 6b–f). Co-bombardment of the *PHO1*-GFP construct with the endoplasmic reticulum (ER) marker ER-rk-mCherry (Nelson *et al.*, 2007) or the late endosomal marker RabF2a-mCherry (Geldner *et al.*, 2009) (Figure 6b,d) did not result in significant overlap between the green and red fluorescent signals. Co-expression of *PHO1*-GFP together with the Golgi markers Got1p-mCherry or Rab2Db-mCherry revealed co-localization of the red and green fluorescent signals (Figure 6c,f), while co-bombardment with the TGN marker VTI12-mCherry only showed partial co-localization (Figure 6e) (Geldner *et al.*, 2009).

To further assess subcellular localization of *PHO1*, a *PHO1*-GFP construct was co-infiltrated into tobacco leaves together with markers of the Golgi and TGN using *A. tumefaciens* mediated transient expression (Grefen *et al.*, 2010). We selected the markers VTI12-mCherry and Syp61-RFP for the TGN, and Got1p-mCherry and Man1-RFP for the Golgi (Langhans *et al.*, 2011). Transient expression of *PHO1*-GFP in tobacco epidermal cells (Figure 7a,d, g, j) resulted in a punctate mobile pattern of fluorescent signal similar to that obtained in Arabidopsis lines functionally expressing *PHO1*-GFP in vascular tissues (Figure 6a). Likewise, the presence of both large and small bodies was observed (Figure 7a,d,g,j). The larger bodies had a mean Feret diameter of 0.97 μm (SD = 0.13 μm , $n = 21$), comparable with the size of larger bodies identified in Arabidopsis lines expressing *PHO1*-GFP. In agreement with the results of onion co-bombardment experiments, a clear overlap between *PHO1*-GFP expression in the larger bodies and Golgi-localized markers Got1p-mCherry and Man1-RFP was observed (Figure 7d–i). Furthermore, in both approaches, the presence of a number of bodies that were only expressing *PHO1*-GFP and neither of the Golgi markers was notable (Figure 6c and 7f, i). Compared with Golgi markers, *PHO1*-GFP co-localized with TGN markers to a much lesser extent (Figure 7a–c,j–l). However, it was noticeable that the

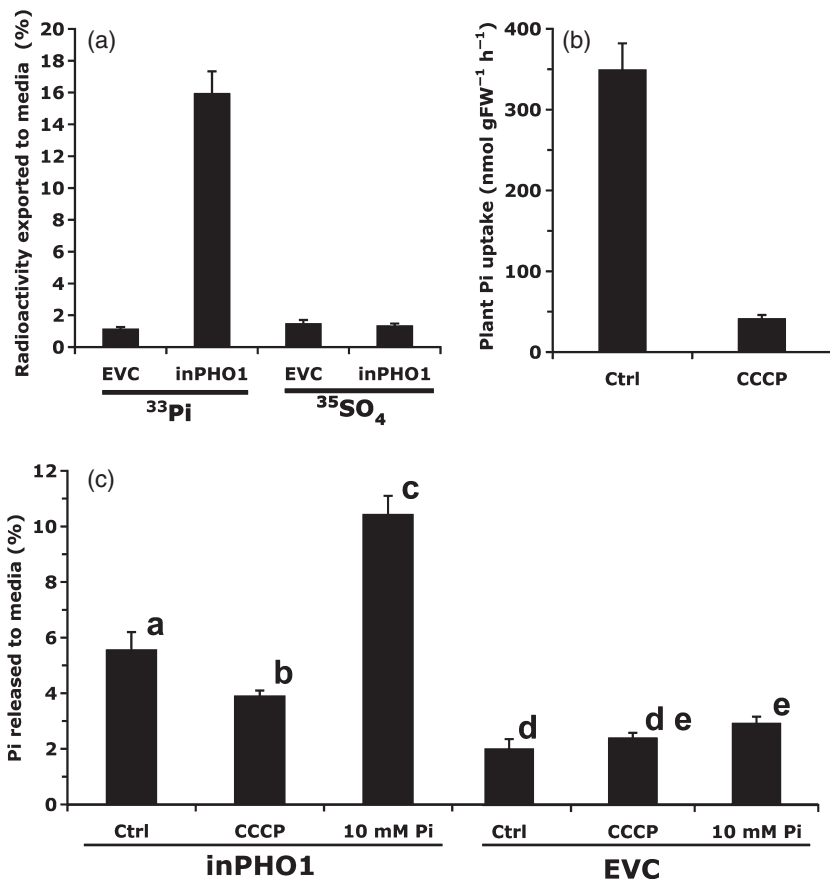


Figure 5. Dynamic of export of inorganic phosphate ($^{33}\text{P}_i$) induced by *PHO1*.

(a) Plants from the empty vector control (EVC) and *PHO1*-inducible (inPHO1#1) lines grown in liquid medium containing $^{33}\text{P}_i$ and $^{35}\text{SO}_4$ were treated with $10\ \mu\text{M}$ estradiol and the net amount of $^{33}\text{P}_i$ and $^{35}\text{SO}_4$ released to the medium was measured after 12 h.

(b) Measurement of Pi uptake into 10-day-old inPHO1#1 seedlings treated with or without (Ctrl) $20\ \mu\text{M}$ carbonyl cyanide *m*-chlorophenylhydraz-one (CCCP) for 1 h.

(c) Plants from the EVC (right panel) and inPHO1#1 (left panel) lines grown in liquid medium containing $^{33}\text{P}_i$ were induced with $10\ \mu\text{M}$ estradiol for 5 h. Plants were then washed, transferred to medium containing $10\ \mu\text{M}$ estradiol and either $50\ \mu\text{M}$ Pi (Ctrl), $50\ \mu\text{M}$ Pi and $20\ \mu\text{M}$ CCCP, or $10\ \text{mM}$ Pi, and net $^{33}\text{P}_i$ export was measured after 1 h. Error bars represent standard deviation ($n = 5$). Values marked with a lowercase letter (a–e) were statistically significantly different from those for other groups marked with different letters ($P < 0.05$, ANOVA, Tukey–Kramer honestly significant difference test).

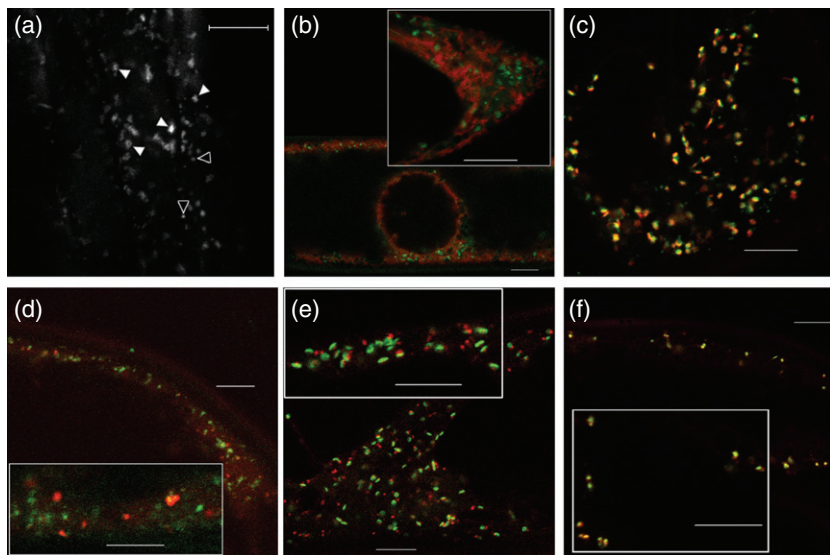


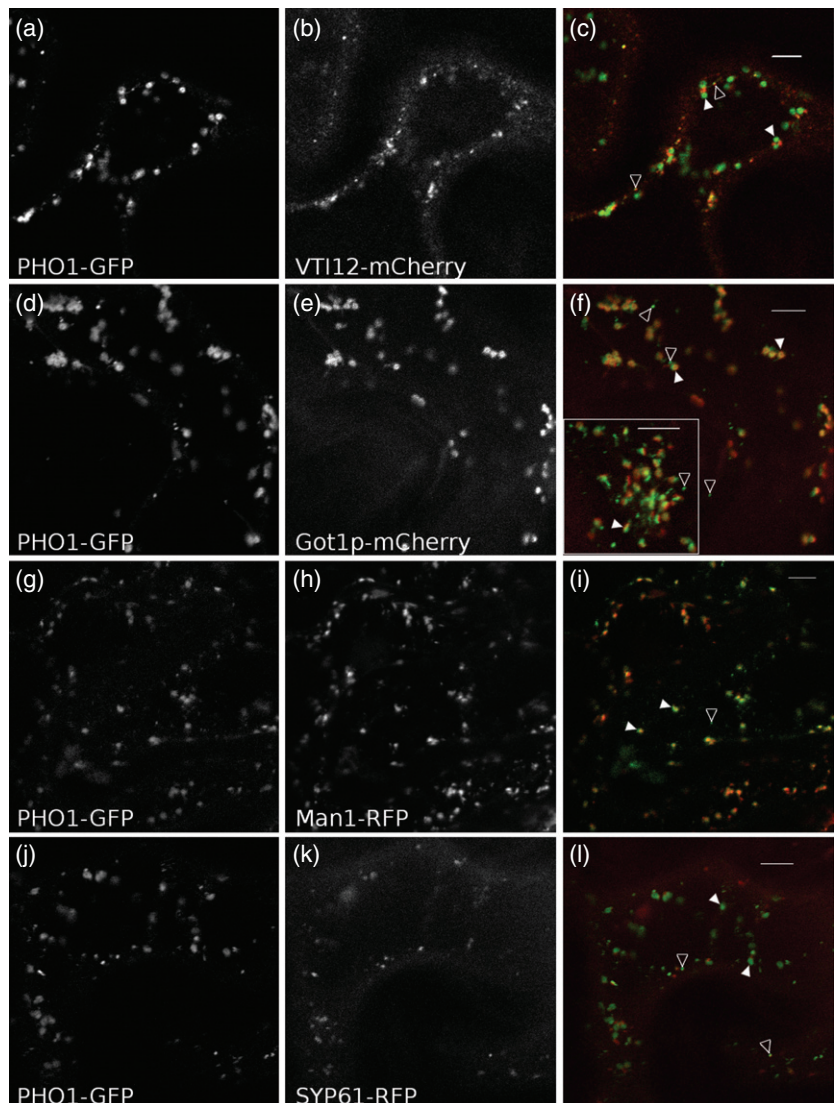
Figure 6. Subcellular localization of *PHO1*-GFP in Arabidopsis and co-expression of *PHO1*-GFP with different markers in onion cells. (a) Expression of *PHO1*-GFP reporter under the *PHO1* promoter in root vascular tissues of 5-day-old Arabidopsis plants. Pericycle cells show most fluorescent foci. Open and closed arrowheads indicate examples of small and large vesicles, respectively. Onion epidermis was co-bombarded with *PHO1*-GFP (b–e) and endoplasmic reticulum (ER) marker ER-rk-mCherry (b), Golgi markers Got1p-mCherry (c) and Rab2Db-mCherry (f), late endosomal marker RabF2a-mCherry (d) and *trans*-Golgi network marker VTI12-mCherry (e). Scale-bars = $10\ \mu\text{m}$. Intensity correlation coefficients (Pearson) were (Rr \pm SE): (b) 0.088 ± 0.003 ; (c) 0.77 ± 0.05 ; (d) 0.134 ± 0.008 ; (e) 0.183 ± 0.006 ; (f) 0.86 ± 0.05 .

co-localized punctate signal corresponded to a fraction of the small-sized vesicle-like structures rather than the disk-shaped larger bodies, which are presumably Golgi bodies. We thus conclude that *PHO1* is localized in the Golgi and extended into the TGN, as well as in vesicular structures of unknown identity.

Effect of brefeldin A on *PHO1*-mediated efflux of Pi in tobacco epidermal cells

Since induction of *PHO1* in Arabidopsis leaves and mesophyll protoplasts led to specific efflux of Pi out of cells, and the *PHO1*-GFP construct was functional in complementing

Figure 7. Co-expression of PHO1-GFP construct with different subcellular markers in tobacco epidermis. Tobacco leaves were co-infiltrated with an *Agrobacterium tumefaciens* strain harboring PHO1-GFP encoding plasmid together with other containing VTI12-mCherry (a–c), Got1p-mCherry (d–f), Man1-RFP (g–i) and Syp61-RFP (j–l). Green and red fluorescence are displayed at the left and in the middle of the row, respectively. Green-colored GFP and red-colored m-Cherry channels are merged at the right. Open and closed arrowheads indicate examples of small and large vesicles, respectively. The inset within (f) depicts an overlay image from another cell. Scale-bars = 10 μ m. Intensity correlation coefficients (Pearson) were ($Rr \pm SE$): (c) 0.47 ± 0.02 ; (f) 0.71 ± 0.02 ; (i) 0.64 ± 0.04 ; (l) 0.144 ± 0.006 .



the *A. thaliana* *pho1* mutant, we tested whether transient expression of the *PHO1-GFP* construct in tobacco leaves could also induce a similar export of Pi from the leaf tissue. While disks cut out from leaves expressing PHO1-GFP exported a large amount of Pi to the bathing medium, representing 38% of the total internal Pi content, disks cut out from buffer-infiltrated (control) and GFP-infiltrated leaves showed only low Pi export, equivalent to approximately 7% of the total internal Pi content (Figure 8a). The Pi efflux was specific, as nitrate efflux was essentially the same for all treatments (Figure 8a), and did not depend on the initial Pi content of the leaf disks used for efflux assay (Figure 8b). Thus, transient expression of the PHO-GFP fusion protein in tobacco led to a specific Pi export out of leaves.

The PHO1-mediated Pi efflux from the tobacco leaves enabled us to test the effect of drugs inhibiting vesicle trafficking on the subcellular localization of PHO1-GFP

fusion protein and the Pi efflux. Among such drugs, wortmannin, a phosphatidylinositol 3-kinase inhibitor (Dasilva *et al.*, 2006), as well as tyrphostins A23 and A51, tyrosine analogs inhibiting the recruitment of endocytic cargo into the clathrin-mediated pathway (Ortiz-Zapater *et al.*, 2006; Dhonukshe *et al.*, 2007), did not have any visible or measurable effect on trafficking of PHO1-GFP or PHO1-mediated Pi efflux, respectively (data not shown). Application of the fungal macrocyclic lactone brefeldin A (BFA), a vesicle trafficking inhibitor, to tobacco leaves leads to the redistribution of Golgi membranes and luminal contents into the ER (Nebenfuhr *et al.*, 2002). We pre-treated the leaves with 70 μ M cycloheximide (CHX) for 30 min before treatment with BFA to prevent the accumulation of newly synthesized proteins which cannot exit the ER (Langhans *et al.*, 2011). Pre-treatment with CHX did not affect either the localization of fluorescent markers fused to

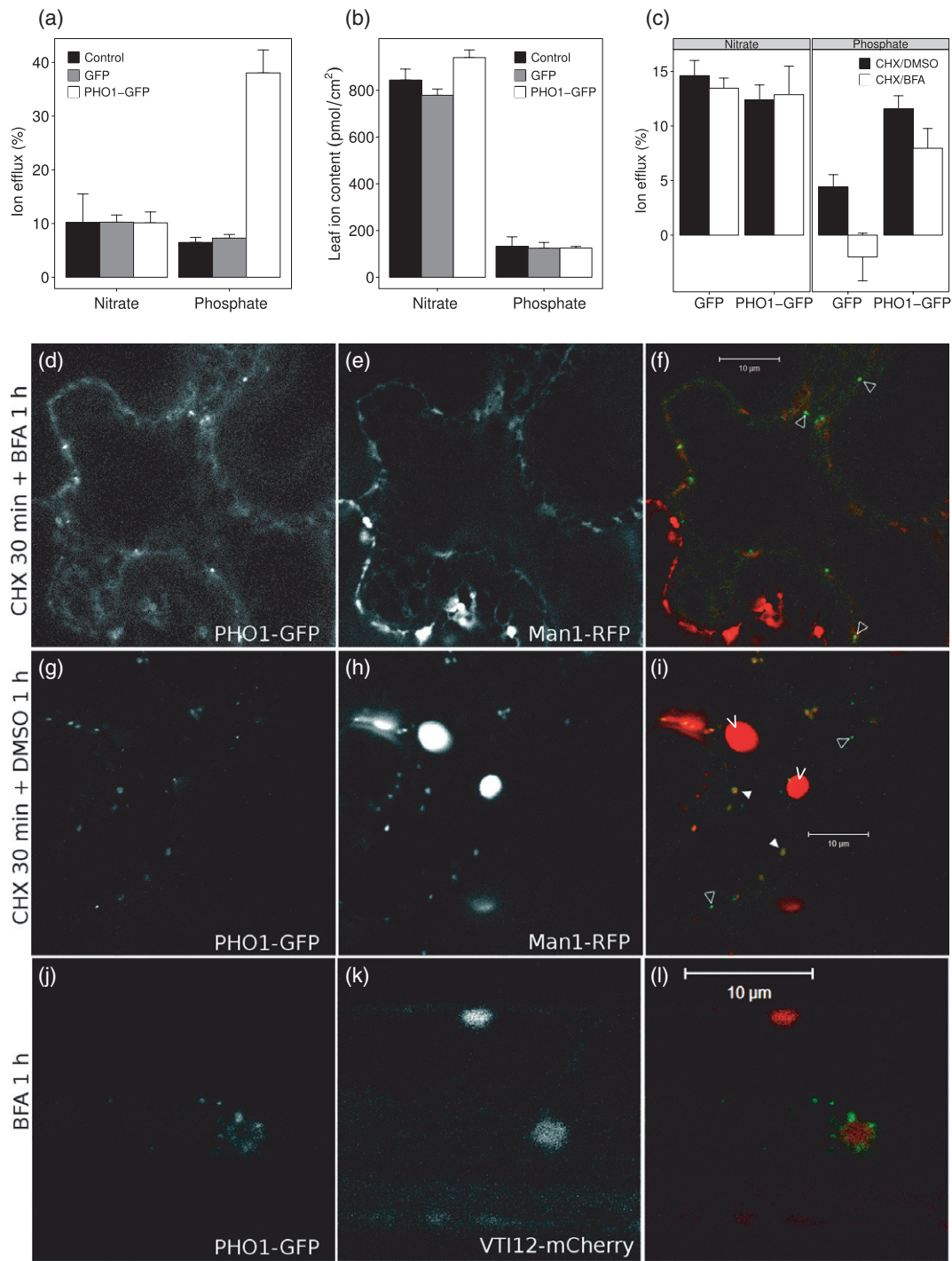


Figure 8. Effect of brefeldin A (BFA) on subcellular localization of PHO1-GFP and PHO1-mediated efflux of inorganic phosphate (Pi). (a) Export of nitrate and phosphate out of disks cut from tobacco leaves infiltrated with buffer (Control) or *Agrobacterium tumefaciens* strains containing GFP or PHO1-GFP constructs, expressed as percentage of total nitrate or phosphate, respectively, contained in the disks. (b) Average phosphate content in the leaf disks used in (a) expressed as picomoles of Pi/cm². (c) Effect of 1 h treatment with 50 μM BFA (or DMSO control) following 30-min pre-treatment with 70 μM cycloheximide (CHX) on efflux of nitrate or phosphate from a disk transiently expressing GFP or PHO1-GFP. Treatments were carried out by infiltrating the solutions into leaves by a syringe, cutting same sized disks (three or four disks per leaf) and immersing them into treatment buffer. Efflux of ions was measured after incubation in perfusion media for 1 h. Effect of BFA (d–f) or DMSO (g–i) treatment on subcellular localization of PHO1-GFP (d, g) and Man1-RFP (e, h). Randomly chosen leaf disks from (c) were analyzed with confocal microscopy. (j)–(l) Effect of 1-h treatment with 50 μM BFA on subcellular localization of PHO1-GFP (j) and VTI12-mCherry (k) in the root vascular tissues of 3-week-old *Arabidopsis* plants grown in soil under a day/night cycle of 16 h/8 h. Green and red colored signals from GFP and RFP or mCherry, respectively, were overlaid for comparison (f, i and l). Open and closed arrowheads indicate examples of small and large vesicles, respectively, while chloroplasts are indicated by a V. Scale-bars represent 10 μm. Intensity correlation coefficients (Pearson) were (Rr ± SE): (f) 0.24 ± 0.01; (i) 0.77 ± 0.03; (k) 0.36 ± 0.06.

PHO1 or Man1 or PHO1-mediated Pi efflux (data not shown). Application of 50 μM BFA to tobacco leaves co-infiltrated with PHO1-GFP and Man1-RFP effectively caused the disappearance of the typical disk-like signal of Golgi-localized Man1-RFP and completely redistributed it to the ER (Figure 8e,h). Similarly, most of the PHO1-GFP signal was also altered by BFA treatment into a diffuse fluorescence that co-localized with the Man1-RFP signal that had been redistributed to the ER (Figure 8d,f), compared with control treatment (Figure 8g,i). However, some intense punctate signal remained in the GFP channel corresponding to small vesicles containing PHO1-GFP but not Man1-RFP (Figure 8F), revealing a population of vesicles that are insensitive to BFA. Interestingly, PHO1-mediated Pi efflux was reduced but remained significantly higher than GFP control samples after the 1 h treatment with 50 μM BFA that effectively caused redistribution of Golgi into the ER (Figure 8c), revealing that Pi export mediated by PHO1 was not strictly dependent on its localization at the Golgi. The BFA treatment did not alter nitrate efflux in either GFP- or PHO1-GFP expressing tobacco leaves (Figure 8c).

While co-localization of the PHO1-GFP signal in the roots of *Arabidopsis* with Wave markers under a range of different physiological conditions failed (see above), upon treatment of 3-week-old *Arabidopsis* roots co-expressing PHO1-GFP and VTI12-mCherry chimeric proteins with 50 μM BFA for 1 h, structures marked with both fluorescent proteins started to aggregate to form the so-called BFA compartments (Figure 8j-l). While the TGN marker was found predominantly in the center of the BFA compartments, punctate signal of PHO1-GFP joined the aggregate mostly peripherally (Figure 8l). This fluorescence pattern is consistent with a predominant localization of PHO1-GFP in the Golgi (Langhans *et al.*, 2011). Thus, consistent with the tobacco epidermis experiments, PHO1-GFP was sensitive to BFA in *Arabidopsis* roots.

Plasma membrane localization of PHO1 in transiently transformed tobacco leaves

The possibility that PHO1, under certain conditions, could also be localized to the PM was investigated. Since increasing the external Pi concentration from 50 μM to 10 mM led to a two-fold increase in PHO1-mediated Pi export (Figure 5c), we tested whether a higher external Pi concentration could affect the dynamics of PHO1 localization. When tobacco leaves transiently expressing PHO1-GFP were infiltrated with perfusion media containing 20 mM KH_2PO_4 for 20 min, a new PHO1-GFP signal emerged overlapping with the signal from the PM marker CBL1-OFP (Batistić *et al.*, 2010), but not when KH_2PO_4 was replaced with KCl to account for changes in extracellular potassium and ionic strength (Figure 9d-i). Under the same conditions, cytosolic GFP expression could be differentiated from the PM signal (Figure 9a-c). Thus, while PHO1 is largely localized to the

Golgi and TGN under normal Pi status, a significant relocalization to the PM can be triggered by high extracellular Pi.

DISCUSSION

We have made use of a construct in which PHO1 expression is inducible by estradiol in order to study the effect of its overexpression in ectopic cells that are otherwise in a normal physiological state before induction. *PHO1* expression in *Arabidopsis* rosette leaves or in whole seedlings clearly showed that export of Pi can be initiated in plants that otherwise have a normal Pi status and growth phenotype. Similar results were also obtained in tobacco leaves transiently expressing a PHO1-GFP fusion protein. Export of Pi was not associated with changes in the export of either nitrate or sulfate. Furthermore, the export of Pi observed following induction of PHO1 in *Arabidopsis* leaf mesophyll protoplasts demonstrates that PHO1-mediated Pi export can occur in cells that are not typically associated with such export. Export of Pi triggered by PHO1 expression was rapid, occurring as early as 2 h after induction, indicating that it is unlikely to be the result of a secondary transcriptional activation of other genes. Together, these results strongly indicate that PHO1 is itself a Pi exporter.

While import of Pi into the cell is tightly coupled to entry of H^+ and dependent on a H^+ gradient across the PM, the relatively weak effect of the proton uncoupler CCCP on PHO1-mediated Pi export indicates that Pi export is largely independent of the H^+ gradient across the PM. Further analysis of PHO1-mediated export of Pi is required to determine whether Pi export is electrogenic and coupled or not to the movement of other cations to maintain a charge balance.

Prolonged induction of PHO1 over-expression over several days leads to poor growth and an associated reduction of Pi in tissues. The decrease in shoot Pi content is explained by the reduction of both root uptake and root-to-shoot translocation of Pi upon induction of PHO1. The overall negative effects of PHO1 over-expression are most likely due to the uncontrolled export of Pi in both roots and shoots and the resulting metabolic costs of maintaining a futile cycle of Pi import and export in a broad spectrum of cells. Such negative effects of uncontrolled PHO1 expression also most likely explain the failure of previous attempts to establish lines over-expressing PHO1 using the CaMV35S promoter (Stefanovic *et al.*, 2011).

The expression in *Arabidopsis* of a functional *PHO1-GFP* construct under the control of the endogenous *PHO1* promoter showed that PHO1 was not localized at the PM but rather in punctate bodies. Similar results were also obtained in onion cells and tobacco leaves. While technical limitations made it impossible to identify these structures in the *Arabidopsis* root pericycle cells, co-localization performed in onion and tobacco both revealed that PHO1 is primarily associated with the Golgi and a population of

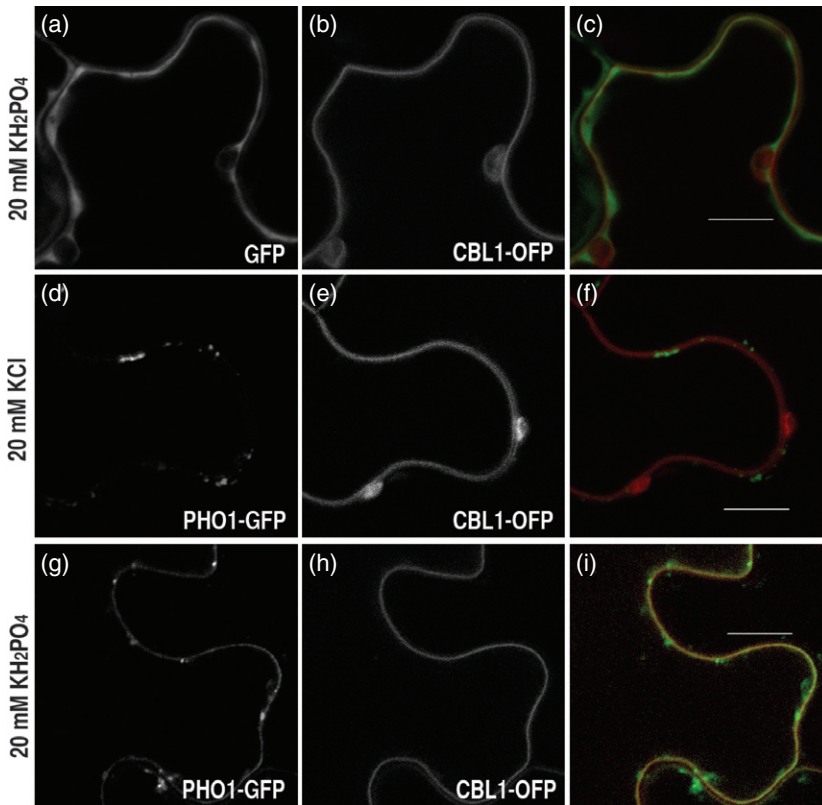


Figure 9. Detection of PHO1-GFP expression at the plasma membrane (PM). Tobacco leaves infiltrated with *Agrobacterium tumefaciens* containing the PM marker CBL1-OFP together with either GFP (a–c) or PHO1-GFP (d–i) constructs. After 48 h, leaves were infiltrated with media containing either 20 mM KH_2PO_4 (a–c,g–i) or 20 mM KCl (d–f) and examined by confocal microscopy 20 min later. Green and red colored signals from GFP and orange fluorescent protein, respectively, were overlaid for comparison (c,f,i). Samples were mounted in the same solution used for treatment (KH_2PO_4 or KCl solution). Scale-bars represent 10 μm . Intensity correlation coefficients (Pearson) were ($R_r \pm \text{SE}$): (c) 0.38 ± 0.02 ; (f) -0.033 ± 0.002 ; (i) 0.34 ± 0.02 .

small bodies partially overlapping with the TGN. Importantly, this pattern of PHO1 expression in infiltrated tobacco leaves was associated with Pi export, indicating that the PHO1-GFP protein was functional in tobacco and thus expressed in the proper subcellular compartments required for Pi export. Interestingly, although treatment of tobacco leaves with BFA led to the expected inhibition of protein transit from the ER to the Golgi, Pi export was itself only weakly reduced by BFA. While the PHO1-GFP signal associated with Golgi was redistributed to the ER in BFA-treated cells, some PHO1-GFP signal associated with small vesicles still remained after BFA treatment.

The absence of PHO1-GFP at the PM and its presence in the Golgi and TGN raises interesting questions as to how PHO1 can mediate the release of Pi to the extracellular space. It remains possible that, at steady-state level, only a minor fraction of PHO1 is localized at the PM and that it is this minor fraction that is responsible for Pi export. While BFA treatment would reduce the transfer of PHO1 from the secretory system to the PM, Pi export could be maintained from the population of PHO1 already present at the PM. A similar situation has recently been described for IRT1, the high-affinity iron transporter responsible for the import of reduced iron from the extracellular space into roots (Barberon *et al.*, 2011). IRT1 is primarily localized in the TGN/early endosomes of root hair cells and no signal at the PM can be detected unless recycling of IRT1 from the PM to endosomes

or multi-vesicular bodies was inhibited by tyrphostin A23 or by blocking monoubiquitination (Barberon *et al.*, 2011). Interestingly, stabilization of IRT1 at the PM was associated with severe iron toxicity. Thus while iron uptake occurs at the PM, the pool of IRT1 located at the PM is very low and kept under tight control to maintain iron homeostasis. Although treatment of tobacco leaves with tyrphostin A23 did not lead to a change in PHO1 localization, PHO1 could be stabilized to the PM by infiltrating high concentration of Pi into leaves. These results reveal that the distribution of PHO1 between the secretory system and the PM can be influenced by Pi homeostasis. Thus, while under most conditions the proportion of PHO1 at the PM would be kept very low, conditions that would increase the cytosolic Pi concentrations, such as those encountered under a high external Pi supply, would favor PHO1 stabilization at the PM to ensure greater Pi export. This model would fit with the observation that high extracellular Pi resulted in increased Pi export in Arabidopsis plants over-expressing PHO1. The influence of external Pi on PHO1 localization is reminiscent of the regulation of the internalization and vacuolar breakdown of the *S. cerevisiae* H^+ -Pi co-transporter PHO84 by the Pi concentration of the medium (Lagerstedt *et al.*, 2002).

An alternative hypothesis to explain the lack of PHO1 at the PM under most conditions is that Pi export would be first mediated by PHO1 loading Pi into endosomes, followed by release of Pi to the extracellular space via exocytosis and

rapid recycling of PHO1 away from the PM. In this model, PHO1-mediated Pi transport would essentially occur in endosomes and not at the PM. Yet, infiltration with high phosphate may slow down PHO1 recycling, leading to a greater proportion being retained at the PM. The lack of strong effect of BFA treatment on Pi export would be explained by the observation that while BFA treatment strongly affects protein transit from the ER to Golgi, a population of vesicles containing PHO1-GFP and capable of mediating loading of Pi into vesicles was insensitive to BFA treatment under our experimental conditions. Such a secretory pathway-mediated mechanism for ion export has previously been hypothesized for the Arabidopsis manganese transporter AtMTP11 (Peiter *et al.*, 2007). AtMTP11 has been localized to the TGN or pre-vacuolar compartment (Delhaize *et al.*, 2007; Peiter *et al.*, 2007). AtMTP11 mediates manganese transport when expressed in yeast and complements the manganese transport and tolerance phenotype of the yeast *pmr1* mutant, deficient in the Golgi-localized Mn^{+2} and Ca^{+2} transporter PMR1 (Lapinskas *et al.*, 1995). The Arabidopsis *mtp11* is hypersensitive to elevated levels of manganese and accumulates more manganese in its tissues, while plants over-expressing AtMTP11 are hypertolerant to manganese (Delhaize *et al.*, 2007; Peiter *et al.*, 2007). Thus, although, manganese export mediated by MTP11 overexpression has not yet been demonstrated, data on AtMTP11 are at least consistent with the action of a transporter acting to load Mn^{+2} into a *trans*-Golgi vesicle. Whether such Mn^{+2} -containing vesicles release their cargo to the extracellular and/or vacuolar space via vesicular fusion remains to be demonstrated.

A growing number of proteins implicated in ion transport are associated with the Golgi and endosomes, including the TGN, which is itself an endosomal compartment (Dettmer *et al.*, 2006). These include AtCLCf and AtCLCd, two members of the chloride channel family (von der Fecht-Bartenbach *et al.*, 2007; Marmagne *et al.*, 2007), the vacuolar H^{+} -ATPase subunit VHA-a1 (Krebs *et al.*, 2010), the Na^{+}/H^{+} antiporters LeNHX2, AtNHX5 and AtNHX6 (Venema *et al.*, 2003; Bassil *et al.*, 2011), the cation/ H^{+} exchangers CHX17, CHX18 and CHX19 (Chanroj *et al.*, 2011), and the P2A-type ATPase AtECA3 involved in Mn^{+2} and Ca^{+2} transport (Li *et al.*, 2008; Mills *et al.*, 2008). PHT4;6 is one member of the PHT4 Pi transporter family that is located in the Golgi, while others are localized to the plastid (Roth *et al.*, 2004; Guo *et al.*, 2008; Cubero *et al.*, 2009). It was postulated that PHT4;6 transport Pi out of the Golgi luminal space for the recycling of Pi released from nucleotide-diphosphate sugars used for protein glycosylation in the Golgi apparatus, although direct evidence for such a function is currently lacking (Cubero *et al.*, 2009).

Altogether, our results on PHO1-mediated Pi export and its localization to the Golgi and TGN highlight a role for the Golgi and associated endosomes in the regulation of Pi

export, an essential component of Pi homeostasis in multicellular eukaryotes (plants and animals) for which PHO1 remains the only known key contributor so far.

EXPERIMENTAL PROCEDURES

Plant material and growth conditions

Plants over-expressing *PHO1* were in the Landsberg *erecta* (Ler) background, while plants expressing the *PHO1-GFP* construct were in the *pho1-2* mutant background (Columbia accession). Plants grown in liquid half-strength MS medium with 1% sucrose were placed on a shaking platform at 100 r.p.m. in a growth room at 22°C under a continuous light intensity of 100 $\mu\text{mol m}^{-2} \text{sec}^{-1}$. Plants in soil were grown under a day/night cycle of 10 h/14 h or 16 h/8 h with a light intensity of 150 $\mu\text{mol m}^{-2} \text{sec}^{-1}$, with day and night temperatures of 22 and 18°C, respectively. *Nicotiana benthamiana* was grown in a greenhouse under a 12-h day/night cycle at 28/22°C and 60% air humidity. Protoplasts were prepared from 4-week-old Arabidopsis leaves as previously described (Abel and Theologis, 1994). For transient expression of PHO1 in tobacco, leaves were infiltrated with *A. tumefaciens*-carrying clones of interest and the suppressor helper component–proteinase (Hc-Pro) (Ma *et al.*, 2009; Grefen *et al.*, 2010).

The DNA construct

For the inducible expression of *PHO1*, the PHO1 genomic coding region from start to stop was amplified by PCR and the 5.4-kb amplicon was cloned into pMDC221 using the Gateway technology (Invitrogen, <http://www.invitrogen.com/>) (Brand *et al.*, 2006). All clones were confirmed by sequencing, introduced into *A. tumefaciens* pGV3101 and transformed into the *A. thaliana* pMDC150-35S activator line (Brand *et al.*, 2006). Controlled expression of *PHO1* in transgenic plants containing the inducible *PHO1* construct was achieved using 5 μM 17- β -estradiol (Sigma-Aldrich, <http://www.sigmaaldrich.com/>) as described earlier (Brand *et al.*, 2006).

The *PHO1-GFP* construct used for complementation of the *pho1-4* mutant was made by amplifying a fragment encoding 2 kbp of the *PHO1* promoter and the complete genomic region coding for *PHO1* without a stop codon. The PCR fragment was cloned into pMDC111 to generate a PHO1-GFP fusion protein (Curtis and Grossniklaus, 2003). For expression of fusion between PHO1 and GFP in onion cells, the complete genomic region coding for *PHO1* was amplified without a stop codon and inserted into the vector pMDC84 (Curtis and Grossniklaus, 2003). All T-DNA vectors were transformed into *A. thaliana* by the floral dip method (Clough and Bent, 1998).

Quantification of Pi and nitrate and Pi transport assay

For the determination of the Pi and nitrate content in plant tissues and mesophyll protoplasts, the cellular content of cells were first released into distilled water or growth media without Pi and/or nitrate by repeated freeze–thaw cycles followed by incubation at 70°C for 30 min. The concentration of Pi in the solution was then quantified by the molybdate assay (Ames, 1966). Nitrate was quantified using either the sulfamic acid method (Carvalho *et al.*, 1998) or according to Barthes *et al.* (1995) scaling down the assay volume 10-fold for the 96-well plate format. The latter was used for samples containing 0.01% Triton X-100. Measurement of the rate of ^{33}P transfer from root to shoot was carried out in plants grown in agar-solidified medium essentially as previously described (Poirier *et al.*, 1991).

Total RNA extraction, RT-PCR and quantitative RT-PCR

The RNA was prepared according to a LiCl protocol (Sambrook and Russel, 2001). For RT-PCR, the amplification reaction were done

with the following primer pairs: *PHO1*, 5'-TAA GGA GAT GGT GGG ACG AA-3' and 5'-TTA ACC GTC TGA GTC CCT GTC-3'; β -tubulin (*TUB6*), 5'-ACC ACT CCT AGC TTT GGT GAT CTG-3' and 5'-AGG TTC ACT GCG AGC TTC CTC A-3'. Real-time quantitative RT-PCR (qPCR) analysis was performed with a Stratagene Mpx3000 instrument (Stratagene, <http://www.genomics.agilent.com/>) according to the standard curve method (Rutledge and Cote, 2003). The *PHO1* amplicon was amplified with 5'-ACA CCA TTC CAG GCA TCC TCC TC-3' and 5'-ACG GTG AGC AAA CAA TCT TCC GC-3' primers. Calculated expression values were normalized against expression levels of the reference gene *At5g46630* (Czechowski *et al.*, 2005).

Protein extracts were prepared from homogenized plant material by extraction in 80 mM 2-amino-2-(hydroxymethyl)-1,3-propanediol (TRIS) pH 8.0, 1 mM EDTA, 5 mM DTT, 1% (v/v) Triton X-100, 10% (v/v) glycerol and 1 mM phenylmethylsulfonyl fluoride (PMSF). For western blotting analysis, 50 μ g of total protein was loaded and run on the SDS-PAGE and transferred to 0.2 μ m nitrocellulose membranes gel according to standard procedures (Sambrook and Russel, 2001). Blots were developed using the ECL Western Blotting Detection Kit (GE Healthcare Biosciences, <http://www.gelifesciences.com/>).

Phosphate, nitrate and sulfate efflux experiments

Efflux of Pi and nitrate from whole leaves was quantified for plants grown in soil for 3–4 weeks under continuous light. Rosette leaves were cut and the major vein removed with a razor blade. The leaf pieces were placed in a tube containing 5 ml of ice-cold medium with 5 mM glucose, 1 mM KCl, 0.5 mM CaCl₂, 0.5 mM MgSO₄, 10 μ M Ca(NO₃)₂ and 20 μ M KH₂PO₄ at pH 5.7 and infiltrated under a mild vacuum over ice for 30 min. After infiltration, the cold medium was replaced with the room-temperature medium and samples placed on the shaker (40 r.p.m.) at 22°C. Aliquots were taken at different time intervals. For measurements in tobacco plants, leaf disks were treated similarly with the exception of addition of 0.01% Triton X-100 to the perfusion media. The phosphate or nitrate content was calculated as the fraction of Pi or nitrate released in the media over the total amount of Pi or nitrate contained in the plant tissue at time zero.

A Pi export assay in whole plants was done with plants grown in liquid MS medium with 1% sucrose for 10 days, followed by transfer to a medium containing 1% sucrose, 10 mM KNO₃, 0.5 mM Ca(NO₃)₂, 0.5 mM MgSO₄ and 0.5 g l⁻¹ 2-(*N*-morpholine)-ethanesulfonic acid (MES) (final pH 5.6) and adding either 5 μ M estradiol or mock treatment. Experiments done with ³³Pi or ³⁵SO₄ were performed similarly, except that 10-day-old plants grown in MS medium with 1% sucrose were transferred to Pi- or SO₄-free media containing 10 μ Ci of ³³Pi or 10 μ Ci of ³⁵SO₄ for 12 h, followed by a wash in non-radioactive media before initiating the export assay in medium containing 1% sucrose, 10 mM KNO₃, 0.5 mM Ca(NO₃)₂, 0.5 mM MgSO₄, 0.5 g l⁻¹ MES (final pH 5.6) and either 50 μ M or 10 mM of KH₂PO₄. The proton ionophore CCCP (Sigma) was used at a final concentration of 20 μ M.

Localization of PHO1-GFP

Co-localization of PHO1-GFP with various subcellular markers was done using constructs and plant lines containing the markers Got1p-mCherry (Wave18R), Rab2Db-mCherry (Wave33R), RabF2a-mCherry (Wave7R) and VTI12-mCherry (Wave13R) previously described (Geldner *et al.*, 2009). Quantification of co-localization was performed using the intensity correlation analysis method implemented in the IMAGEJ plugin of the MBF IMAGEJ bundle (<http://www.macbiophotonics.ca/imagej/>). For this analysis, regions of interest (ROIs) were selected when necessary to exclude plastids.

For particle bombardment of onion epidermis, tungsten micro-carriers (1 μ m) coated with plasmid DNA (1.7 μ g mg⁻¹ microcarrier) were bombarded on onion scales using a custom-made ballistic system. Microscopy was performed using a Zeiss LSM 700 confocal microscope with a C-Apochromat 63 \times /1.20 objective (Zeiss, <http://www.zeiss.co.uk/>).

ACKNOWLEDGEMENTS

The authors are very grateful to Niko Geldner for helpful discussion and to J. Kudla, D. Robinson and K. Schumacher for providing markers for the PM, TGN and Golgi. This work was funded by grants 3100A-122493 and 3100A-138339 to YP. The authors declare no conflict of interest.

SUPPORTING INFORMATION

Additional supporting information may be found in the online version of this article:

Figure S1. The inducible *PHO1* construct.

Figure S2. Export of inorganic phosphate (pP) in plants over-expressing *PHO1*.

Figure S3. Complementation of *pho1-2* by *PHO1-GFP*.

Figure S4. Fluorescence pattern of *PHO1-GFP* in *pho1-2*.

Please note: As a service to our authors and readers, this journal provides supporting information supplied by the authors. Such materials are peer-reviewed and may be organized for online delivery, but are not copy-edited or typeset. Technical support issues arising from supporting information (other than missing files) should be addressed to the authors.

REFERENCES

- Abel, S. and Theologis, A. (1994) Transient transformation of Arabidopsis leaf protoplasts: a versatile experimental system to study gene expression. *Plant J.* **5**, 421–427.
- Ames, B.N. (1966) Assay of inorganic phosphate, total phosphate and phosphatases. *Methods Enzymol.* **8**, 115–118.
- Barberon, M., Zelazny, E., Robert, S., Conéjéro, G., Curie, C., Friml, J. and Vert, G. (2011) Monoubiquitin-dependent endocytosis of the IRON-REGULATED TRANSPORTER 1 (IRT1) transporter controls iron uptake in plants. *Proc. Natl Acad. Sci. USA* **108**, E450–E458.
- Barthes, L., Bousser, A., Hoarau, J. and Deleens, E. (1995) Reassessment of the relationship between nitrogen supply and xylem exudation in detopped maize seedlings. *Plant Physiol. Biochem.* **33**, 173–183.
- Bassil, E., Ohto, M.-A., Esumi, T., Tajima, H., Zhu, Z., Cagnac, O., Belonte, M., Peleg, Z., Yamaguchi, T. and Blumwald, E. (2011) The Arabidopsis intracellular Na⁺/H⁺ antiporter NHX5 and NHX6 are endosome associated and necessary for plant growth and development. *Plant Cell* **23**, 224–239.
- Batistić, O., Waadt, R., Steinhorst, L., Held, K. and Kudla, J. (2010) CBL-mediated targeting of CIPKs facilitates the decoding of calcium signals emanating from distinct cellular stores. *Plant J.* **61**, 211–222.
- Bonfante, P. and Genre, A. (2010) Mechanisms underlying beneficial plant-fungus interactions in mycorrhizal symbiosis. *Nature Commun.* **1**, 1–10. doi:10.1038/ncomms1046.
- Brand, L., Horler, M., Nuesch, E., Vassalli, S., Barrell, P., Yang, W., Jefferson, R.A., Grossniklaus, U. and Curtis, M.D. (2006) A versatile and reliable two-component system for tissue-specific gene induction in Arabidopsis. *Plant Physiol.* **141**, 1194–1204.
- Bucher, M. (2006) Functional biology of plant phosphate uptake at root and mycorrhiza interfaces. *New Phytol.* **173**, 11–26.
- Carvalho, A., Meireles, L. and Malcata, F. (1998) Rapid spectrophotometric determination of nitrates and nitrites in marine aqueous culture media. *Analisis* **26**, 347–351.
- Chanroj, S., Lu, Y., Padmanaban, S., Nanatani, K., Uozumi, N., Rao, R. and Sze, H. (2011) Plant-specific cation/H⁺ exchanger 17 and its homologs are endomembrane K⁺ transporters with roles in protein sorting. *J. Biol. Chem.* **286**, 33931–33941.
- Chiou, T.-J. and Lin, S.-I. (2011) Signaling network in sensing phosphate availability. *Ann. Rev. Plant Biol.* **62**, 185–206.

- Clough, S.J. and Bent, A.F. (1998) Floral dip: a simplified method for *Agrobacterium*-mediated transformation of *Arabidopsis thaliana*. *Plant J.* **6**, 735–743.
- Cubero, B., Nakagawa, Y., Jiang, X.Y., Miura, K.J., Li, F., Raghothama, K.G., Bressan, R.A., Hasegawa, P.M. and Pardo, J.M. (2009) The phosphate transporter PHT4;6 is a determinant of salt tolerance that is localized to the golgi apparatus of *Arabidopsis*. *Mol. Plant-Microbe Interact.* **2**, 535–552.
- Curtis, M.D. and Grossniklaus, U. (2003) A gateway cloning vectors set for high-throughput functional analysis of genes in plants. *Plant Physiol.* **133**, 462–469.
- Czechowski, T., Stitt, M., Altmann, T., Udvardi, M. and Scheible, W. (2005) Genome-wide identification and testing of superior reference genes for transcript normalization in *Arabidopsis*. *Plant Physiol.* **139**, 5–17.
- Dasilva, L., Foresti, O. and Denecke, J. (2006) Targeting of the plant vacuolar sorting receptor BP80 is dependent on multiple sorting signals in the cytosolic tail. *Plant Cell*, **18**, 1477–1497.
- Delhaize, E., Gruber, B., Pittman, J.K., White, R., Leung, H., Miao, Y., Jiang, L., Ryan, P. and Richardson, A. (2007) A role for the AtMTP11 gene of *Arabidopsis* in manganese transport and tolerance. *Plant J.* **51**, 198–210.
- Detmer, J., Hong-Hermesdorf, A., Stierhof, Y.D. and Schumacher, K. (2006) Vacuolar H⁺-ATPase activity is required for endocytic and secretory trafficking in *Arabidopsis*. *Plant Cell*, **18**, 715–730.
- Dhonukshe, P., Aniento, F., Hwang, I., Robinson, D., Mravec, J., Stierhof, Y. and Friml, J. (2007) Clathrin-mediated constitutive endocytosis of PIN auxin efflux carriers in *Arabidopsis*. *Curr. Biol.* **17**, 520–527.
- von der Fecht-Bartenbach, J., Bogner, M., Krebs, M., Stierhof, Y.-D., Schumacher, K. and Ludewig, U. (2007) Function of the anion transporter AtCLC-d in the trans-Golgi network. *Plant J.* **50**, 466–474.
- Gaymard, F., Pilot, G., Lacombe, B., Bouchez, D., Bruneau, D., Boucherez, J., Michaux-Ferrière, N., Thibaud, J.-B. and Sentenac, H. (1998) Identification and disruption of a plant shaker-like outward channel involved in K⁺ release into the xylem sap. *Cell*, **94**, 647–655.
- Geldner, N., Dénervaud-Tendon, V., Hyman, D.L., Mayer, U., Stierhof, Y.D. and Chory, J. (2009) Rapid, combinatorial analysis of membrane compartments in intact plants with a multicolor marker set. *Plant J.* **59**, 169–178.
- Grefen, C., Donald, N., Hashimoto, K., Kudla, J., Schumacher, K. and Blatt, M. (2010) A ubiquitin-10 promoter-based vector set for fluorescent protein tagging facilitates temporal stability and native protein distribution in transient and stable expression studies. *Plant J.* **64**, 355–365.
- Guo, B., Jin, Y.H., Wussler, C., Blancaflor, E.B., Motes, C.M. and Versaw, W.K. (2008) Functional analysis of the *Arabidopsis* PHT4 family of intracellular phosphate transporters. *New Phytol.* **177**, 889–898.
- Hamburger, D., Rezzonico, E., MacDonald-Comber, P., Petétot, J., Somerville, C. and Poirier, Y. (2002) Identification and characterization of the *Arabidopsis* PHO1 gene involved in phosphate loading to the xylem. *Plant Cell*, **14**, 889–902.
- Krebs, M., Beyhl, D., Görllich, E., Al-Rasheid, K.S., NMarten, I., Stierhof, Y.D., Hedrich, R. and Schumacher, K. (2010) *Arabidopsis* V-ATPase activity at the tonoplast is required for efficient nutrient storage but not for sodium accumulation. *Proc. Natl Acad. Sci. USA*, **107**, 3251–3256.
- Lagerstedt, J.O., Zvyagilskaya, R., Pratt, J.R., Pattison-Granberg, J., Kruckeberg, A.L., Berden, J.A. and Persson, B.L. (2002) Mutagenic and functional analysis of the C-terminus of *Saccharomyces cerevisiae* Pho84 phosphate transporter. *FEBS Lett.* **526**, 31–37.
- Langhans, M., Forster, S., Helmchen, G. and Robinson, D. (2011) Differential effects of the brefeldin A analogue (6R)-hydroxy-BFA in tobacco and *Arabidopsis*. *J. Exp. Bot.* **62**, 2949–2957.
- Lapinskas, P., Cunningham, K., Liu, X., Fink, G. and Culotta, V. (1995) Mutations in PMR1 suppress oxidative damage in yeast cells lacking superoxide dismutase. *Mol. Cell. Biol.* **15**, 1382–1388.
- Li, X., Chanroj, S., Wu, Z., Romanowsky, S.M., Harper, J.F. and Sze, H. (2008) A distinct endosomal Ca²⁺/Mn²⁺ pump affects root growth through the secretory process. *Plant Physiol.* **147**, 1675–1689.
- Lin, S.H., Kuo, H.F., Canivenc, G. et al. (2008) Mutation of the *Arabidopsis* NTR1.5 nitrate transporter causes defective root-to-shoot nitrate transport. *Plant Cell*, **20**, 2514–2528.
- Ma, P., Liu, J., He, H., Yang, M., Li, M., Zhu, X. and Wang, X. (2009) A viral suppressor P1/HC-Pro increases the GFP gene expression in *Agrobacterium*-mediated transient assay. *Appl. Biochem. Biotechnol.* **158**, 243–252.
- Marmagne, A., Vinauger-Douard, M., Monachello, D., Falcon de Longevialle, A., XCharon, C., Allot, M., Rappaport, F., Wollman, F.-A., Barbier-Brygoo, H. and Ephritikhine, G. (2007) Two members of the *Arabidopsis* CLC (chloride channel) family, AtCLCe and AtCLCf, are associated with thylakoid and Golgi membranes, respectively. *J. Exp. Bot.* **58**, 3385–3393.
- McLean, B.G., Hempel, F.D. and Zambryski, P.C. (1997) Plant intercellular communication via plasmodesmata. *Plant Cell*, **9**, 1043–1054.
- Mills, R.F., Doherty, M.L., Lopez-Marqués, R.L., Weimar, T., Dupree, P., Palgren, M.G., Pittman, J.K. and Williams, L.E. (2008) ECA3, a Golgi-localized P2A-type ATPase, plays a crucial role in manganese nutrition in *Arabidopsis*. *Plant Physiol.* **146**, 116–128.
- Nebenfuhr, A., Ritzenthaler, C. and Robinson, D. (2002) Brefeldin A: Deciphering an enigmatic inhibitor of secretion. *Plant Physiol.* **130**, 1102–1108.
- Nelson, B.K., Cai, X. and Nebenfuhr, A. (2007) A multicolored set of in vivo organelle markers for co-localization studies in *Arabidopsis* and other plants. *Plant J.* **51**, 1126–1136.
- Ortiz-Zapater, E., Soriano-Ortega, E., Marcote, M., Ortiz-Masia, D. and Aniento, F. (2006) Trafficking of the human transferrin receptor in plant cells: effects of tyrphostin A23 and brefeldin A. *Plant J.* **48**, 757–770.
- Peiter, E., Montanini, B., Gobert, A., Pedas, P., Husted, S., Maathuis, F.J.M., Blaudez, D., Chalot, M. and Sanders, D. (2007) A secretory pathway-localized cation diffusion facilitator confers plant manganese tolerance. *Proc. Natl Acad. Sci. USA*, **104**, 8532–8537.
- Poirier, Y. and Bucher, M. (2002) Phosphate transport and homeostasis in *Arabidopsis*. In *The Arabidopsis Book* (Somerville, C.R. and Meyerowitz, E.M., eds). Rockville, MD: American Society of Plant Biologists. 1–35.
- Poirier, Y., Thoma, S., Somerville, C. and Schiefelbein, J. (1991) A mutant of *Arabidopsis* deficient in xylem loading of phosphate. *Plant Physiol.* **97**, 1087–1093.
- Roth, C., Menzel, G., Petetot, J., Rochat-Hacker, S. and Poirier, Y. (2004) Characterization of a protein of the plastid inner envelope having homology to animal inorganic phosphate, chloride and organic-anion transporters. *Planta*, **218**, 406–416.
- Rutledge, R.G. and Cote, C. (2003) Mathematics of quantitative kinetic PCR and the application of standard curves. *Nucleic Acid Res.* **31**, e93.
- Sambrook, J. and Russel, D. (2001) *Molecular cloning, a laboratory manual*. Cold Spring Harbor, USA: Cold Spring Harbor Laboratory Press.
- Secco, D., Baumann, A. and Poirier, Y. (2010) Characterization of the rice PHO1 gene family reveals a key role for *OsPHO1;2* in phosphate homeostasis and the evolution of a distinct clade in dicotyledons. *Plant Physiol.* **152**, 1693–1704.
- Secco, D., Wang, C., Arpat, B.A., Wang, Z., Poirier, Y., Tyerman, S.D., Wu, P., Shou, H. and Whelan, J. (2012) The emerging importance of the SPX domain-containing proteins in phosphate homeostasis. *New Phytol.* **193**, 852–841.
- Stefanovic, A., Arpat, A.B., Bligny, R., Gout, E., Vidoudez, C., Bensimon, M. and Poirier, Y. (2011) Overexpression of PHO1 in *Arabidopsis* leaves reveals its role in mediating phosphate efflux. *Plant J.* **66**, 689–699.
- Takano, J., Noguchi, K., Yasumori, M., Kobayashi, M., Gajdos, Z., Miwa, K., Hayashi, H., Yoneyama, T. and Fujiwara, T. (2002) *Arabidopsis* boron transporter for xylem loading. *Nature*, **420**, 337–340.
- Venema, K., Belver, A., Marin-Manzano, M.M., Rodriguez-Rosales, M.P. and Donaire, R.P. (2003) A novel intracellular K⁺/H⁺ antiporter related to Na⁺/H⁺ antiporters is important for K⁺ ion homeostasis in plants. *J. Biol. Chem.* **278**, 22453–22459.
- Wang, Y., Ribot, C., Rezzonico, E. and Poirier, Y. (2004) Structure and expression profile of the *Arabidopsis* PHO1 gene family indicates a broad role in inorganic phosphate homeostasis. *Plant Physiol.* **135**, 400–411.
- Wang, Y., Secco, D. and Poirier, Y. (2008) Characterization of the PHO1 gene family and the responses to phosphate deficiency of *Physcomitrella patens*. *Plant Physiol.* **146**, 646–656.